PROTOTYPE TESTS OF THE ELECTROMAGNETIC PARTICLE INJECTOR CONCEPT DEMONSTRATE ITS PRIMARY ADVANTAGES FOR FAST TIME RESPONSE DISRUPTION MITIGATION IN TOKAMAKS

R. RAMAN
University of Washington
Seattle, WA, USA
email: raman@aa.washington.edu

S.C. JARDIN
Princeton Plasma Physics Laboratory
Princeton, NJ, USA

C. CLAUSER
Princeton Plasma Physics Laboratory
Princeton, NJ, USA

R. LUNSFORD
Princeton Plasma Physics Laboratory
Princeton, NJ, USA

J.E. MENARD
Princeton Plasma Physics Laboratory
Princeton, NJ, USA

M. ONO
Princeton Plasma Physics Laboratory
Princeton, NJ, USA

Abstract

Predicting and controlling disruptions is an important and urgent issue for ITER. Some disruptions with a short warning time may be unavoidable. For these cases, a fast time response disruption mitigation method is essential. Experimental tests on a prototype system of a novel, rapid time-response disruption mitigation system (DMS) being developed as a backup option for ITER, referred to as the Electromagnetic Particle Injector (EPI), has been able to verify the primary advantages of the concept, which are its ability to meet short warning time scales of <10 ms while attaining the projected high velocities for deep radiative payload penetration in ITER-scale plasmas. Because the ITER plasma would have about two orders of magnitude more energy than in present experiments and with a much more energetic edge region, realistic 3d MHD simulations, benchmarked against current experiments, are necessary to project to ITER. In support of this requirement, new capabilities have been implemented in the M3D-C1 code to model radiative material injection into tokamak plasmas, and initial simulations for the NSTX-U configuration have been conducted. The EPI relies on an electromagnetic propulsion system to overcome the limitations of present gas-based systems, such as Shattered Pellet Injection (SPI), limited to 200 m/s for large mass pellets. A metallic sabot is accelerated electromagnetically to the required velocities (> 1 km/s) within 2 ms, at which point it releases well-defined microspheres, or a shell pellet, of a radiative payload. Initial experimental tests from the prototype system show attainment of over 600 m/s in about 1 ms. Essential aspects of payload separation from the sabot and sabot capture have also been demonstrated at 150 m/s, and the method can be extended to over 2 km/s.

1. INTRODUCTION

The Electromagnetic Particle Injector (EPI) is a novel fast time response system for tokamak disruption mitigation. It is being proposed as a backup option for disruption mitigation in ITER. Disruption mitigation in tokamaks is achieved by injecting a radiative payload deep into the tokamak plasma. The EPI has the potential for delivering the radiative payload to the plasma center on a <10 ms time scale, much faster and deeper than what can be achieved using present methods. Predicting and controlling disruptions is an important and urgent issue for ITER. While a primary focus is the early prediction and avoidance of conditions favourable to a disruption, it is understood that some disruptions may be inescapable. For these cases, a fast-time response method is essential to protect the ITER facility. Experimental tests on a prototype system have been able to verify the predicted rapid response capability of the EPI system by accelerating a 2 g sabot to 600 m/s in 1 ms.

The EPI concept's primary advantage over present systems is its ability to meet short warning time scales while

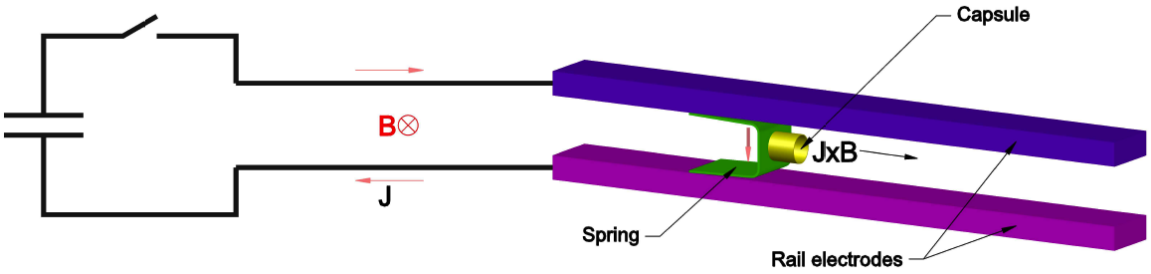

FIG. 1. Cartoon showing the EPI electrical circuit, EPI electrodes, the sabot, and the chamber that would contain the radiative payload. A JxB interaction between the current through the sabot and the magnetic field between the rails accelerates the sabot.

accurately delivering a radiative payload to the plasma core. This is done at velocities required to achieve core penetration in high power ITER discharges, thus providing thermal and runaway current mitigation. The EPI system described here overcomes the physics limitations of present gas-based disruption mitigation systems by relying on an electromagnetic propulsion system for pellet acceleration, as illustrated in Fig. 1. The EPI system accelerates a metallic capsule, termed a sabot, to high velocity within 2 ms. At the end of its acceleration, the sabot releases a payload of radiative granules of a known velocity and distribution. Alternately it could also release a shell pellet containing smaller pellets or noble gas. Previous studies have indicated the system's capability to both respond on a 1-2 ms time-scale and achieve 1 km/s velocities [1].

It is helpful to note that at present, MGI (Massive Gas Injection) and Shattered Pellet Injection (SPI) are the most tested methods for disruption mitigation in present tokamaks [2 ,3]. The MGI method [4] relies on a fast-acting gas valve that empties a high-pressure plenum, filled with high-z gas, into the plasma discharge. Due to limitations such as, for example, high radiation fields that exist near a reactor vessel, the valve needs to be located some distance away from the vessel [5]. On ITER, this is many meters away from the plasma.

The Shattered Pellet [6] injection system accelerates a frozen high-z gas such as argon, neon, deuterium, or some combination of these gases using a high-pressure gas pulse from an MGI valve to propel the pellet. Before injection into the plasma discharge, the pellet is fragmented, and smaller fragments are injected into the vessel.

Because of the use of gases in the MGI system, or for SPI propulsion, or present shell pellet propulsion, the propellant gas limits the pellet velocity to about 300-400 m/s [7] Consequently, the projected response time for the MGI system on ITER is about 40 ms, and over 30 ms for the Shattered Pellet system [8].

SPI fragments' limited velocity may also make it difficult for SPI fragments to penetrate adequately deep into an ITER-scale plasma. To have an idea of how deep these pellets could penetrate in high-power ITER plasma, simulations were conducted for penetration into ITER-like profiles representative of a 350 MJ, 15 MA ITER H-mode discharge. The ORNL pellet injection code [9] was used for these simulations. The injection was assumed to be purely radial, and from the device mid-plane location as this would result in the deepest possible penetration. The ITER discharge profiles were obtained from ASTRA simulations carried out by Polevoi [10]. The results are shown in Fig. 11 in Ref [12]. It is important to note that these single pellet injections do not model the penetration of SPI fragments as in the case of SPI, numerous fragments entering the plasma would tend to cool the plasma edge, thus permitting deeper penetration of the fragments, but they do indicate the challenges for pellet penetration in high-power plasmas. The figure shows that neither of the two simulated neon pellets (2 mm or 1 mm in diameter) would be able to reach the q = 2 surface. These are typical of neon shard sizes resulting from a fragmented neon pellet [11]. The much higher edge temperature and density of the ITER plasma cause these small, low-velocity pellets to ablate near the plasma periphery. In comparison, such pellets would be able to propagate to the q = 2 surface on DIII-D sized plasmas [12], raising the question of how well results from present experiments could be used to project to ITER reliably. Thus, reliable 3d MHD modelling [13] (validated by experimental studies) is necessary to project to ITER-class plasmas reliably.

The EPI overcomes gas-propelled injectors' issues by relying on a simple electromagnetic propulsion system for solid particle injection, without the simultaneous injection of undesirable propellant gas that could initiate an edge thermal cooling before the primary radiative payload enters the plasma. The higher velocity would allow the

radiative material to be deposited inside the q=2 surface before a thermal quench is initiated, and it has the potential to stop the initiation of runaway electrons.

2. EXPERIMENTAL RESULTS FROM OFF-LINE DEVELOPMENT OF EPI

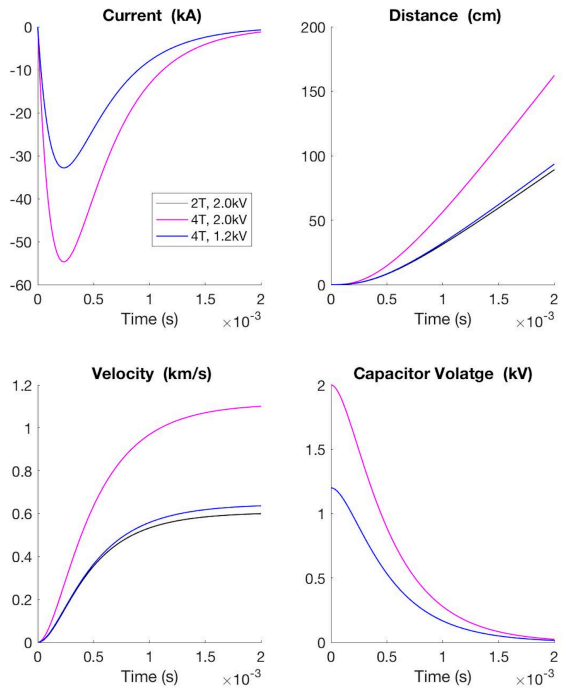

FIG. 2. Calculated parameters for a present tokamak scale experiment.

Motivated by the promising results from the proto-type EPI-1 system [14], work on a much-improved system is in progress. The significant improvement of this system, termed EPI-2, is a present high external boost field capability of at least 3 T, with the potential for a future upgrade to 4 T for a tokamak test in consideration.

The calculated parameters for a near-term tokamak experiment are shown in Fig. 2. From Fig. 2, at an external field of 4 T, operating at a voltage of just 1.2 kV, for a 20 mF capacitor bank, which is the same as that used in the EPI-1 development, routine velocities exceeding 0.5 km/s would be possible. Velocities of 1 km/s will be possible if the operating voltage is increased to 2 kV, which is the same as that used in the EPI-1 tests.

The core components of the EPI-2 system consist of two metal rails measuring 2 cm in height x 0.95 cm wide. They are 58 cm long and are separated from each other by 2 cm. On either side of the rails are 58 cm long, 2 cm high PEEK insulators, followed by a metal block. All these are sandwiched between two flame-resistant and vacuum-compatible insulating sheets that are 0.63 cm in height. In this magnetic field augmentation design, the magnetic field enhancing coils are positioned on the insulating sheets' top and bottom. This entire assembly is compressed using metal plates and other metal bars placed on either side of the boost coils. This core assembly is shown located inside the total system that is shown in Fig. 3.

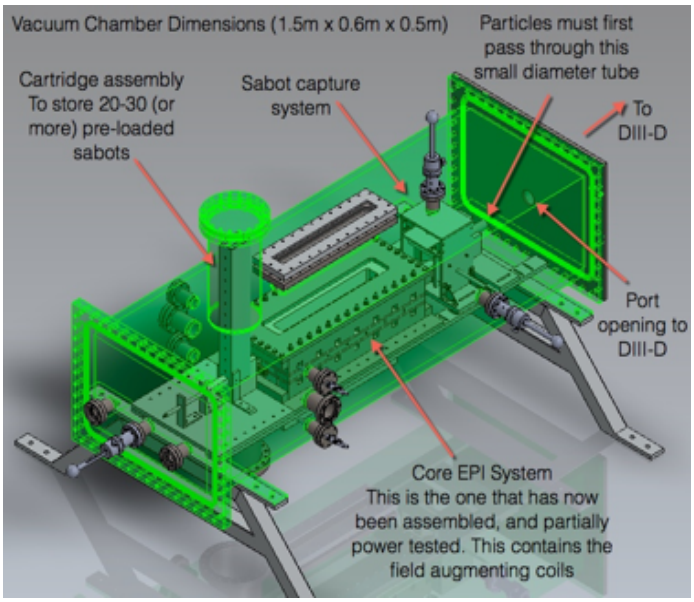

FIG. 3. Guide tube configuration for payload injection into a currently operating tokamak such as DIII-D or KSTAR. The core of the EPI system is located near the center of the vacuum tank. In front of the core assembly is the sabot capture system. Behind the core system is an automatic sabot loading system.

Fig. 3 shows the main vacuum tank that would house the injector, the sabot loading system, and the sabot retrieval system. The overall dimensions are about 0.6 m x 0.7 m x 1.5 m. A small turbopump and an oil-free roughing pump would be used to keep the system under vacuum. The main components inside the vacuum tank are (a) the core injector region that has an electrode acceleration length of 55cm, (b) the sabot loading system that is located behind the core EPI components, and (c) the sabot retrieval system that is located in front of the core EPI hardware. The configuration can store 20 or more sabots and the contained payload. After each discharge, a new sabot could be remotely loaded from the tokamak

Control Room. The sabot loading and removal arms would be composed of pneumatic actuators to perform the needed actions using a control signal from the EPI system controller.

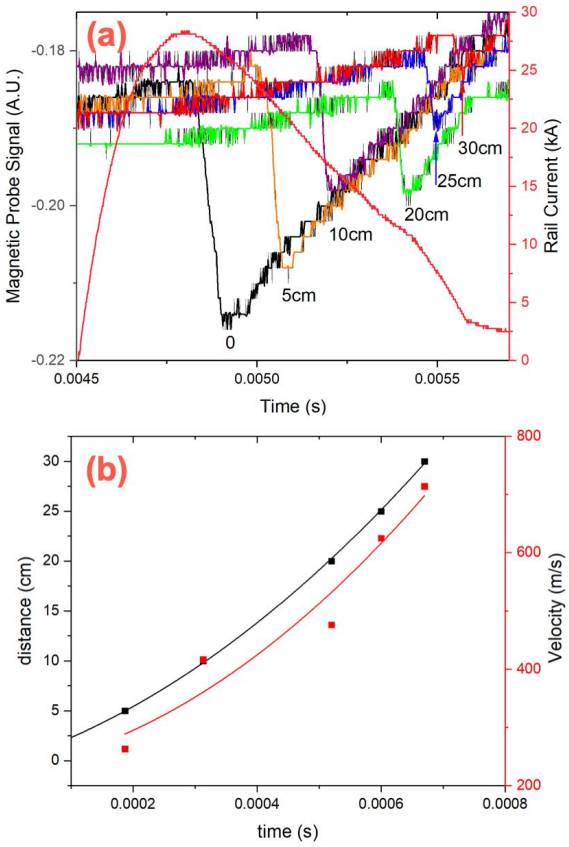

FIG. 4. Experimental results from the off-line testing of the EPI-2 injector. (a) magnetic probe traces along the length of the accelerator show the magnetic flux propagating along the 30 cm length of the injector in about 1 ms. The rail current is 28 kA. (b) The sabot distance and velocity trace for the data in frame (a)

Initial experimental tests from the prototype system (EPI-1) have demonstrated 150 m/s within 1.5 ms, consistent with calculations [14], giving confidence that a larger ITER-scale injector can be developed. Following these successful experiments, a new upgraded system (EPI-2) in a tokamak deployment configuration has been built to increase the velocity to 1 km/s. Initial results from this system's operation at 2.1 T have extended the attainable velocities to over 600 m/s in the same 1.5 ms, consistent with the projections for this system that indicate the attainment of 1 km/s with the use of a 3 T boost magnetic field.

Fig. 4a shows experimental data from the operation of EPI-2. The magnetic field probe traces that record the expanding magnetic flux behind the sabot show continuous acceleration along the 30 cm long acceleration region. The processed data from these signals (Fig. 4b) shows the attainment of over 600 m/s in less than 1 ms. Essential aspects of payload separation from the sabot, and sabot capture have also been demonstrated on EPI-2 at 150 m/s, and the method can be extended to over 2 km/s [15].

3. DEVELOPMENT OF M3D-C1 CAPABILITY FOR EPI

The plasma volume of ITER is 830 m^3, and it is physically much larger than any currently operating tokamak. In comparison, JET has a plasma volume of 100 m^3. Additionally, the ITER plasma would have about two orders of magnitude more energy than in present experiments and with a much more energetic edge region. Thus, one cannot rely solely on experiments in current machines to project to ITER. Reliable and realistic 3d MHD simulations, benchmarked against present experiments, is an essential step to project to ITER confidently. In support of this requirement, new capabilities have been implemented in the M3D-C1 code to model radiative material injection into tokamak plasmas. As a first step towards developing this capability, initial simulations for the NSTX-U configuration have been conducted to model solid particle injections such as those possible in an early tokamak test of the EPI concept.

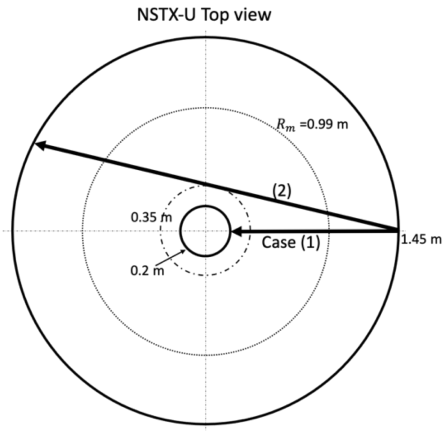

FIG. 5. Top-down view showing the carbon pellet injection geometry. Case 1 is for pure radial injection, which minimizes the pellet propagation time to the magnetic axis. Case 2 is for a shallow injection cases, such as that which is likely to be used in the EPI configuration as in the absence of a plasma, the pellet could leave the vessel through a port at the opposite end of the pellet trajectory. This would avoid the pellet impacting the center stack of the tokamak.

These new capabilities being added to M3D-C1 will also be capable of modelling SPI penetration for ITER. Ablation and radiation capability for the first solid material radiative species implemented in M3D-C1 is carbon [16]. The target plasma configuration used for these simulations for the injection of solid carbon pellets is NSTX-U. The ablation model is based on a neutral gas shielding approach (NGS) [17, 18] in which the key quantity is the shielding factor

$\delta = q_p/q_0$, where q_p is the plasma heat flux that has reached the pellet surface and q_0 is the plasma heat flux before entering the pellet neutral cloud. For both strong ($\delta \ll 1$) and weak ($\delta \lesssim 1$) shielding, analytical expressions can be derived [17,18] and an interpolated expression that covers both limits that has been proposed in Ref [17] was incorporated in M3D-C1.

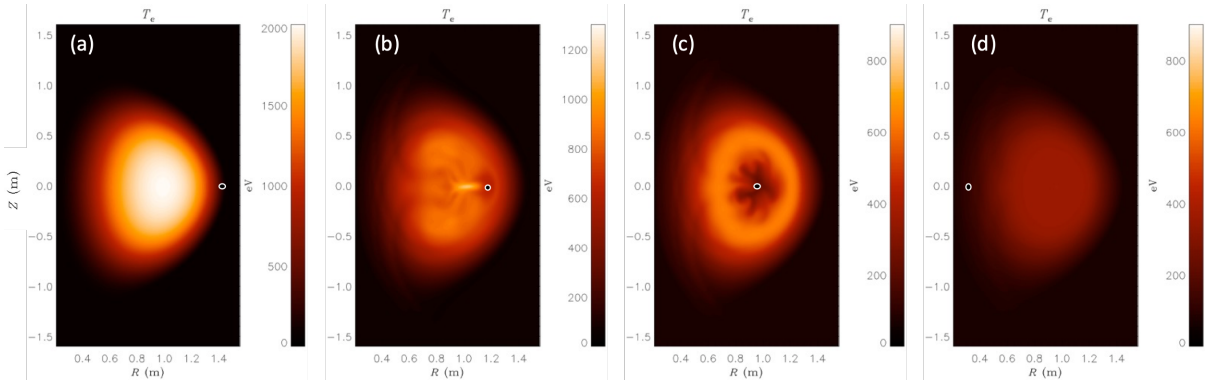

FIG. 6. The plasma electron temperature for different time slices (a-d corresponding to 0, 0.235, 0.438, and 1.09 ms respectively) for the 1000 m/s pellet velocity case injected radially inward. The small circle within the frame shows the pellet position at each time.

In these initial studies a wide range of simulations have been covered by injecting a single spherical carbon pellet and scanning over different modelling parameters. The ablated material was weighted with a gaussian-like shape in both poloidal and toroidal direction. Preliminary scans suggested that a gaussian half-width in the poloidal direction of 5 cm and, approximate a half-width length of 50 cm in the toroidal direction are small enough to allow 3D effects to arise. The code also uses a density diffusion term in the continuity equation for each species that ranged between $2 - 10 \times 10^{-5}$ (internal units) to avoid numerical instabilities. These quantities can be reduced using a finer mesh but that would require much more computational resources being unpractical for convergence studies. Further studies targeted to a particular configuration might have smaller modelling parameters.

To obtain an estimate for the amount of carbon atoms required for a full thermal quench mitigation, a 2D simulation was conducted. This showed that the carbon content in a 2 mm diameter pellet (which contains 3.2×10^{20} atoms) would be enough to mitigate the plasma if all the material is ablated and uniformly deposited within the plasma volume. Here uniformly means that the 2d carbon density profile was set to be proportional to the electron density profile. This pellet size was used in the subsequent 3D simulations. A single pellet was injected from the outer midplane as shown in Fig. 5. For the pure radial inward injection, Case (1), three different injection velocities were used: 1000 m/s, 500 m/s and 300 m/s respectively.

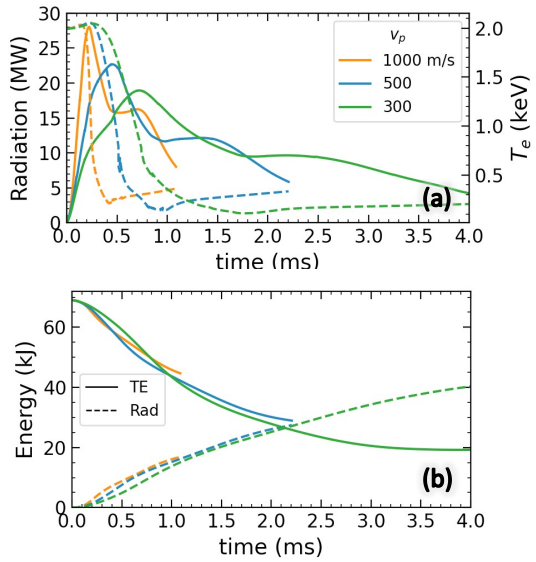

FIG. 7: (Top) Radiated power (solid lines) and T_e (dashed lines) (b) Thermal Energy (TE) is shown by the solid lines and radiated energy by the dashed lines. These are as a function of time for the three injection velocities.

Figure 6 shows the plasma electron temperature for different time slices (a-d) for the 1000 m/s pellet velocity case injected radially inward. The small circle within the frame indicates the pellet position at each time. These frames correspond to times 0.0, 0.235, 0.438, and 1.09 ms respectively.

The plasma response and the thermal collapse due to the pellet ablated material is clearly seen in the 2d temperature plots. At t = 0.0 ms, the pellet is just inside the plasma separatrix. This is the reference starting condition. At t = 0.235 ms, the pellet has propagated to the q = 2.4 surface (r/a = 0.38). The core electron temperature has dropped from about 2 keV to about 1000 eV. At this point the plasma central temperature is falling very sharply. Simulations show that the core flux surfaces are broadening and becoming

partially stochastic. The field lines at the pellet position are now linked to the plasma core but not to the edge. Therefore, the heat flux that balances the pellet radiation is coming primarily from the core and, hence, the plasma temperature becomes hollow. At = 0.438 ms, the pellet has reached the magnetic axis. The electron temperature around the magnetic axis now drops to about 200 eV, but the region surrounding the magnetic axis is at a higher electron temperature of over 500 eV. At this point the stochastization spreads to the edge and therefore the temperature at the center starts rising due to the hotter edge plasma. Finally, in the last frame corresponding to t = 1.09 ms, the pellet is almost exiting the plasma from the inboard side. The resulting plasma has now reformed and has a nearly uniform electron temperature above 250 eV. These sequences of images show that a 2 mm diameter carbon pellet traveling at 1 km/s through a NSTX plasma with a core electron T_e of ~ 2 keV does not fully ablate and a full thermal quench is not attained from the injection of a single pellet of this size.

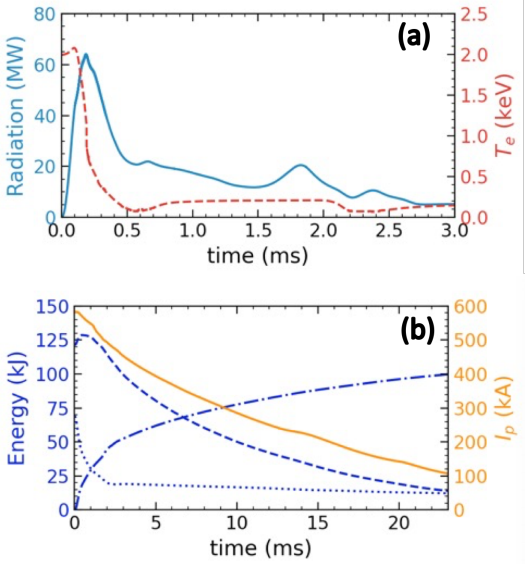

FIG. 8: (a) The total radiated power and the central electron temperature for the case of a tangential shell pellet injection at 1 km/s, for the pellet trajectory shown as Case 2 in Fig. 5. (b) Shown are traces for the plasma current (solid), plasma thermal energy (dotted), plasma magnetic energy (dashed) and total radiated energy (dash-dotted).

Figure 7 shows (a) the radiation power and the plasma central electron temperature, as a function of time for the three scanned velocities. Figure 7 (b) shows the plasma thermal energy and the radiated energy as a function of time. At this early instance the plasma current and magnetic energy are not significantly affected. The total ablated material in these cases ranged from 11% (for 1000 m/s) to 21% (for 300 m/s), leading to a partial thermal quench, as can be noted in Fig 7 (b).

To increase the pellet ablation fraction, as shown in Case 2 of Figure 5, a larger radius pellet and with tangential injection was simulated. M3D-C1 at this time does have the capability to model the simultaneous injection of several small pellets, such as would be the case with SPI injection. The use of a larger diameter pellet is an approximation to an array of smaller pellets since the purpose was to increase the effective surface area to increase the ablation rate. In this case, we used a 7.2 mm diameter pellet. The pellet is hollow, and the shell thickness adjusted, so that the amount of material is the same as in a 2 mm solid spherical pellet. In this sense, the situation would be roughly similar to having ~13 solid pellets of ~0.85 mm each. This case is shown in Fig. 8 for a pellet velocity of 1000 m/s. In this case, the total ablated material was ~32%, showing a significant increase from the previous case. Figure 8(a) shows the radiation power and the plasma central electron temperature during the time the pellet is passing through the plasma. Figure 8(b) shows the plasma current (solid line) the plasma thermal (dotted line), magnetic (dashed line) and radiated (dash-dotted line) energy as a function of time. The simulation ran up to 24 ms. Even though not all the material was ablated, the results show that it was enough to produce a current quench. The observation that these pellets, even those with a velocity of 300 m/s, do not fully ablate gives us confidence that high-velocity pellets may have the potential for penetration well past the q = 2 surface to induce an inside-out thermal quench. Additionally, the partial ablation of carbon suggests that shell pellets may be a good way to transport materials to within the q = 2 surface, especially if they are coated with a material that has a lower ablation rate, such as for example, tungsten for ITER purposes. The present work is being extended to simulating a solid carbon shell pellet containing carbon dust inside it in order to evaluate the plasma response to a large payload that is deposited in the plasma core before a thermal quench is triggered due to material deposited outside the q = 2 surface.

4. CONCLUSIONS

The EPI method to inject high-velocity granules of the required size for ITER discharge termination holds great promise for addressing a critical ITER need. The EPI system accelerates a sabot. The sabot is a metallic capsule that can be accelerated to high velocity by an electromagnetic impeller. At the end of its acceleration, within 2-3 ms, the sabot will release granules of a known velocity and distribution, or a shell pellet containing smaller pellets or noble gas.

The primary advantage of the EPI concept over SPI and other gas propelled systems is its potential to meet short warning time scales while accurately delivering the required particle size and materials at the velocities needed for achieving the required penetration depth in high power ITER discharges. The present understanding is that as little as 5 g of Be may be adequate for both thermal quench and runaway electron mitigation in ITER [19]. This radiative payload must be deposited in the plasma's core (and not at the edge as in present methods such as SPI).

In this proposed method, a radiative payload consisting of microspheres of Be, BN, or B, or other acceptable low-Z materials, or a shell pellet, would be injected into the plasma center for thermal and runaway electron mitigation. The radiative payload would be accelerated to the required velocities (~200-1000 m/s for present tokamaks and ~1 km/s or higher for ITER) by the EPI system. Calculations indicate that the system can attain the required velocities for the granule sizes necessary in less than 1.5 ms after a command is issued to trigger the system. A prototype system has been tested offline to verify the projected system response time and attainable velocities. Both are consistent with the model calculations, giving confidence that larger systems can be built to attain the target ITER goals. An important advantage of the EPI system is that it could be positioned very close to the reactor vessel because it is fully electromagnetic, with no mechanical reusable moving parts. This has the added benefit that if the injector is aligned with the external fields, the performance dramatically increases while simultaneously reducing the payload's transit time from the injector to the tokamak plasma.

The EPI system controls both the particles' size and velocity permitting easier and perhaps more reliable modelling using 3d MHD codes. The ITER DMS requires the level of capabilities offered by the EPI system to ensure the safety of the ITER facility.

ACKNOWLEDGEMENTS

This work is supported by U.S. DOE Contracts: DE-AC02-09CH11466, DE-FG02-99ER54519 AM08, AND DESC0006757REFERENCES

[1] RAMAN, R., JARBOE, T.R.., MENARD, J.E., et al., Fast time response electromagnetic disruption mitigation concept, Fusion Science & Technol., **68** 797, 2015.

[2] WHYTE, D.G., et al., Disruption mitigation with high pressure noble gas injection, Journal of Nuclear Materials, **313-316**, (2003) 1240.

[3] GRANETZ, R.S., et al., Disruption mitigation studies on ALCATOR C-MOD and DIII-D, Nuclear Fusion **47**, 1086 (2007)

[4] BOZHENKOV, S.A., FINKEN, K.-H., LEHNEN, M. and WOLF, R.C., Main characteristics of the fast disruption mitigation valve, Rev. Sci. Instrum., vol. **78**, no. 3, (2007) 033503.

[5] MARUYAMA, S., et al., "ITER fueling and glow discharge cleaning system overview," ITR/P5-24, Proc. 24th IAEA Fusion Energy Conf., San Diego, USA (2012).

[6] SHIRAKI, D., et al., "Thermal quench mitigation and current quench control by injection of mixed species shattered pellets in DIII-D," Phys. of Plasmas **23**, 0625516 (2016)

[7] BAYLOR, L.R., BARBOER, C.C., CARMICHAEL, J.R., et al., "Disruption mitigation system developments and design for ITER," Fusion. Science and Technology **68**, 211 (2015).

[8] LEHNEN, M., ITER Disruption Mitigation Workshop Report, ITER HQ, 8-10 March 2017

[9] HOULBERG W.A., MILORA S.L. and ATTENBERGER S.E. 1998 Neutral and plasma shielding model for pellet ablation Nucl. Fusion 28 595

[10] POLEVOI, A.R., CAMPBELL, D.J., CHUYANOV, A.A. *et al* 2013 Assessment of plasma parameters for the low activation phase of ITER operation, Nucl. Fusion **53** 123026

[11] GEBHART, T.E., BAYLOR, L.R., and MEITNER, S.J., Experimental pellet shatter thresholds and analysis of shatter tube ejecta for disruption mitigation cryogenic pellets, IEEE Trans. Plasma Sci., Vol **48**, No. 6 (2020) 1598

[12] RAMAN, R., SWEENEY, R., MOYER, R.A., et al., "Shattered pellet penetration in low and high energy plasmas on DIII-D," Nucl. Fusion 60 (2020) 036014, https://doi.org/10.1088/1741-4326/ab686f

[13] IZZO, V.A., PARKS, P.B., LAO, L.L. 2009 DIII-D and ITER rapid shutdown with radially uniform deuterium delivery, Plasma Physics and Controlled Fusion **51** 105004

[14] RAMAN, R., LAY, W-S., JARBOE, T.R., MENARD, J.E., ONO, M., Nucl. Fusion **59** (2019) 016021

[15] HOLCOMB, C.T., et al., Review of Scientific Instruments, Vol **72**, No. 1 (2001) 1054

[16] FERRARO, N., LYONS, B., KIM, C., et al, Nucl. Fusion **59** 016001 (2019)

[17] SERGEEV, V. YU., et al., Plasma Phys. Rep. **32** (2006) 363

[18] KUTEEV, B. V., et al., Sov. J. Plasma Phys. **10** (1984) 675

[19] KONAVALOV, S. V. et al., Studying the capabilities of Be pellet injection to mitigate ITER disruptions Proc. IAEAFEC 2012 Conf. (San Diego, USA, 8–13 October) ITR/ P1-38 (www-naweb.iaea.org/napc/physics/FEC/FEC2012/papers/338_ITRP138.pdf)